Timing and intensity of humid interglacial and interstadial periods from the Eemian in the southwestern Mediterranean region: new chronological and stable isotope data from Aït Said ou Idder (Middle Atlas) and comparison with other regional tufa deposits (Morocco and southern Spain)

Julie Dabkowski, Quentin Wackenheim, Christophe Falguères, Denis Fiorillo, Olivier Tombret, Nicole Limondin-Lozouet, Larbi Boudad, Jean-François Berger

E&G Quaternary Sci. J., 71, 45–58, 2022
https://doi.org/10.5194/egqsj-71-45-2022

Open Access E&G Quaternary Science Journal

Research article

Timing and intensity of humid interglacial and interstadial periods from the Eemian in the southwestern Mediterranean region: new chronological and stable isotope data from Aït Said ou Idder (Middle Atlas) and comparison with other regional tufa deposits (Morocco and southern Spain)

Julie Dabkowski[1], Quentin Wackenheim[1,2], Christophe Falguères[3], Denis Fiorillo[4], Olivier Tombret[3], Nicole Limondin-Lozouet[1], Larbi Boudad[5], and Jean-François Berger[6]

[1]Laboratoire de Géographie Physique: environnements quaternaires et actuels (UMR 8591), CNRS – Université Paris 1 Panthéon-Sorbonne – Université Paris-Est Créteil, Meudon, France
[2]Trajectoires (UMR 8215), CNRS – Université Paris 1 Panthéon-Sorbonne, Paris, France
[3]Histoire Naturelle de l'Homme Préhistorique (UMR 7194), CNRS – MNHN, Paris, France
[4]Archéozoologie – Archéobotanique. Sociétés, pratiques et environnements (UMR 7209), CNRS – MNHN, Paris, France
[5]Département de Géologie, Université Mohammed V de Rabat, Rabat, Morocco
[6]Environnement, Ville, Société (UMR 5600, IRG), CNRS – Université de Lyon, Lyon, France

Correspondence: Julie Dabkowski (julie.dabkowski@lgp.cnrs.fr)

Relevant dates: Received: 22 July 2021 – Revised: 3 December 2021 – Accepted: 14 January 2022 – Published: 14 March 2022

How to cite: Dabkowski, J., Wackenheim, Q., Falguères, C., Fiorillo, D., Tombret, O., Limondin-Lozouet, N., Boudad, L., and Berger, J.-F.: Timing and intensity of humid interglacial and interstadial periods from the Eemian in the southwestern Mediterranean region: new chronological and stable isotope data from Aït Said ou Idder (Middle Atlas) and comparison with other regional tufa deposits (Morocco and southern Spain), E&G Quaternary Sci. J., 71, 45–58, https://doi.org/10.5194/egqsj-71-45-2022, 2022.

Abstract: In the last few decades, multidisciplinary research on calcareous tufas as palaeoenvironmental and palaeoclimatic records has intensively grown, which has provided an increasing number of well-documented sites. Consequently, inter-site comparisons and regional- to continental-scale reviews have developed, discussing the link between tufa distribution and climate or providing diachronic comparisons of climatic and environmental conditions prevailing during Quaternary interglacials (and interstadials). This paper proposes such a review for the southeastern Mediterranean area, including new dating and isotopic data from Aït Said ou Idder (northern Morocco) to be compared with available regional data, in order to discuss the intensity of some humid periods of the last 125 kyr.

According to several radiocarbon and U–Th dates, three chronological phases are indeed identified at Aït Said ou Idder: the Holocene, the Dansgaard–Oeschger (D–O) interstadial 8 and the Marine Isotopic Stage (MIS) 5e. Similarly, other tufa deposits from both Morocco and southern Spain (mostly Andalusia) appear to have preferentially developed during interglacial or interstadial periods, marked by maximal developments of the Mediterranean forest as reported in the palynological records from

regional marine cores. Furthermore, isotopic data (δ^{18}O and δ^{13}C) from Aït Said ou Idder (and from other southeastern Mediterranean tufa deposits where available) suggest no significant difference in terms of temperature or air mass circulation between the Holocene, D–O 8 and MIS 5e. In terms of humidity conditions, no evidence of strong aridity is recorded even if D–O 8 appears drier than both interglacials. Conditions seems slightly wetter during the Holocene than during MIS 5e, but δ^{13}C values at Aït Said ou Idder could also reflect strong differences in the seasonality of these interglacials. We demonstrate that calcareous tufa deposits have promising potential for discussing, in both space and time, the climate variability in the southeastern Mediterranean area, but new investigations, including dating and stable isotopes, are required to accurately feed such discussions.

Kurzfassung:

In den letzten Jahrzehnten ist die multidisziplinäre Forschung zur Rolle von Kalktuffen (Tufa) als Paläoumwelt- und Paläoklima-Archiv intensiv ausgebaut worden, wodurch nun eine weiterhin wachsende Zahl gut dokumentierter Standorte vorliegt. Infolgedessen war es im Rahmen von Vergleichen zwischen verschiedenen Standorten und auf der Grundlage vergleichender Bewertungen auf regionalem bis hin zu kontinentalem Maßstab einerseits möglich, den Zusammenhang zwischen der Verteilung von Kalktuffen und Klima zu diskutieren, sowie andererseits diachrone Vergleiche von klimatischen Bedingungen und Umweltbedingungen während der Interglaziale (und Interstadiale) im Quartär durchzuführen. Diese Studie stellt eine solche vergleichende Bewertung für den südöstlichen Mittelmeerraum bereit und präsentiert darüber hinaus neue Datierungen und Isotopen-Daten aus Aït Said ou Idder (nördliches Marokko), die mit vorliegenden regionalen Daten verglichen werden, um somit eine Einschätzung der Intensität ausgewählter humider Abschnitte der letzten 125 kyr vornehmen zu können.

Basierend auf mehreren Radiokohlenstoff- und U–Th-Datierungen können in Aït Said ou Idder drei chronologische Phasen ausgewiesen werden: das Holozän, das Dansgaard/Oeschger Interstadial 8 und das MIS 5e. In ähnlicher Weise scheinen sich andere Kalktuffablagerungen sowohl aus Marokko als auch aus Südspanien (hauptsächlich Andalusien) bevorzugt während solcher Interglazial- oder Interstadialperioden entwickelt zu haben, die basierend auf der palynologischen Auswertung regionaler mariner Bohrkernarchive durch eine maximale Entwicklung mediterraner Wälder gekennzeichnet sind. Darüber hinaus deuten Isotopendaten (δ^{18}O and δ^{13}C) aus Aït Said ou Idder (und aus anderen Kalktuffen des südöstlichen Mittelmeerraumes, sofern verfügbar) darauf hin, dass es keine signifikanten Unterschiede in Bezug auf Temperatur oder Luftmassenzirkulation zwischen dem Holozän, dem D/O 8 und dem MIS 5e gab. Im Hinblick auf die Feuchtigkeitsbedingungen finden sich keine Hinweise starker Aridität, auch wenn das D/O 8 relativ trockener erscheint als beide Interglaziale. Die Bedingungen scheinen während des Holozäns etwas feuchter gewesen zu sein als während des MIS 5e, aber die δ^{13}C-Werte in Aït Said ou Idder könnten auch starke Unterschiede in der Saisonalität dieser Interglaziale widerspiegeln. Unsere Studie zeigt, dass Kalktuffablagerungen ein vielversprechendes Potenzial haben, um die Klimavariabilität im südöstlichen Mittelmeerraum sowohl räumlich als auch zeitlich zu diskutieren, aber neue Untersuchungen, einschließlich Datierungen und Untersuchungen an stabilen Isotopen, sind erforderlich, um diese Diskussion sorgfältig und genau zu untermauern. (*Abstract was translated by Christopher Luethgens.*)

1 Introduction

In the last few decades, multidisciplinary research on calcareous tufas has intensively grown regarding their potential for palaeoenvironmental and palaeoclimatic studies: they are one of the few continental archives to simultaneously provide records of past environments (including fauna and flora) and independent proxies for climatic variations (from calcite stable isotopes) which can also be precisely and objectively dated (Andrews, 2006; Capezzuoli et al., 2014; Dabkowski, 2014). In parallel, as the number of well-documented sites has increased, inter-site comparisons and regional- to continental-scale reviews have developed, either discussing the link between tufa chronological distribution and climate and/or anthropogenisation (e.g. Dabkowski, 2020; Goudie et al., 1993; Ollivier et al., 2006; Pentecost, 1995; Vaudour, 1994; Weisrock, 1986) or providing diachronic comparisons of climatic and environmental conditions prevailing during Quaternary interglacials (Limondin-Lozouet, 2011; Limondin-Lozouet and Preece,

2014; Dabkowski and Limondin-Lozouet, 2021). However, investigations have mostly focused on European tufas so far. In Morocco, reviews on the ages of tufa deposits have been initiated on the basis of U–Th dating (Falguères et al., 2016; Rousseau et al., 2017; Weisrock et al., 2008), but they concerned indurated, well-crystallised deposits (so-called "travertines"), from which palaeoenvironmental and palaeoclimatic data are more difficult to retrieve (Capezzuoli et al., 2014; Dabkowski, 2014). The tufa sequence of Aït Said ou Idder in the Middle Atlas is the first to have recently provided palaeoenvironmental reconstructions based on malacological data (Wackenheim et al., 2020).

This paper proposes to review the climatic significance of tufa deposits in the southeastern Mediterranean area based on their chronological distribution and isotopic signal. It will first present new U–Th dating and isotopic data from Aït Said ou Idder to be compared with available regional data from Morocco and Andalusia in order to discuss the intensity of some humid periods of the last 125 kyr.

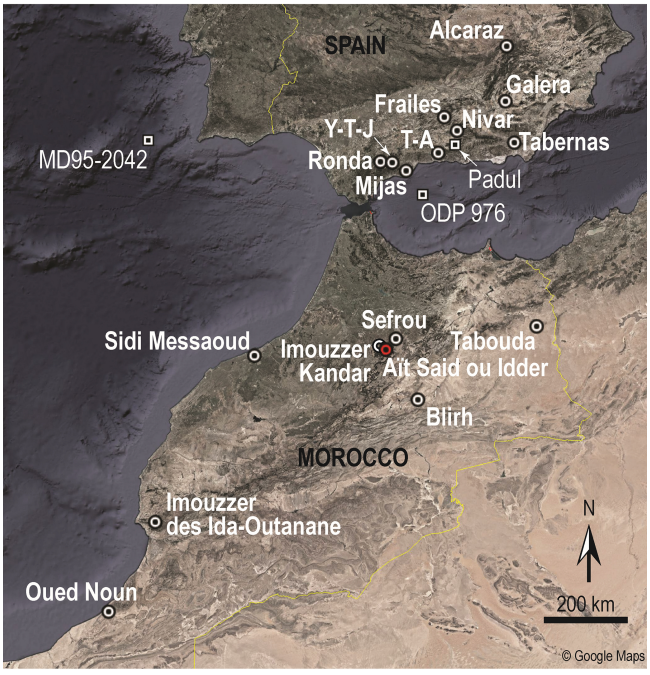

Figure 1. Localisation map of Aït Said ou Idder (red spot) and other tufa deposits discussed in this paper (circles). T–A: Tejeda–Almijara; Y–T–J: Yunquera–Tolox–Jorox. Squares show other palaeoenvironmental or palaeoclimatic records mentioned in the text (background map from © Google Maps, modified by Julie Dabkowski).

2 Studied site and material

The Aït Said ou Idder (ASI) tufa is located in the Middle Atlas, northeast Morocco, about 40 km south of Fez in the vicinity of the Dayet Aoua (33°38′49.50″ N, 4°59′38.33″ E; Fig. 1). The studied profile, ca. 45 m long and 3 to 4 m high, was previously described in detail by Wackenheim et al. (2020). Two main phases of tufa deposition have been observed on the field (Fig. 2). The lower stratigraphical units 10 to 7 are sub-horizontal and characterised by fluvio-paludal facies (Pedley, 1990; Pedley et al., 2003) including large oncoliths and indurated phytoherms (units 10 and 9), silty to sandy stratified levels (unit 8), and a fine mudstone-like whitish unit at the top (unit 7; Fig. 2). No major discontinuity is clearly observed within these lower units in the eastern part of the profile where they are better exposed. However, in the central part, a stepped-shape incision at the top of unit 8 is locally observed, which may correspond to a hiatus between units 8 and 7 (Fig. 2, red line).

The upper part of the unit 7 is then clearly affected by erosive processes, and indurated angular fragments of it are preserved within the base of the overlying unit 6. The following units 6 to 1 show an east-to-west inclination and facies that are typical of slope tufa (Pedley, 1990), namely silty to granular tufa comprising fragments of encrusted vegetation alternating with silty to sandy tufa (Fig. 2). The lowermost unit 6 especially provides burned tufa fragments and millimetric charcoals evidencing a local fire event. These charcoals were large enough to be dated with confidence (see below). The whole ASI sequence, except unit 9 which was too indurated, was sampled for malacology and geochemistry (Fig. 2). The malacological investigations provide detailed palaeoenvironmental reconstructions and allow selecting shells of suitable species to be dated (Wackenheim et al., 2020). The resulting chronological data are summarised in the following section.

3 Chronological data

3.1 Former radiocarbon dating

All the previous dates obtained at ASI were through radiocarbon dating and are summarised in Table 1. Dated material includes three millimetric individual charcoals from unit 6, a bunch of microcharcoals from unit 5, and five bunches of mollusc shells from units 1, 3, 4 and 7 (Table 1 and Fig. 2; Wackenheim et al., 2020). While charcoals from unit 6 were handpicked on the field, the bunch of microcharcoal from unit 5 was subsampled within sedimentological samples under a binocular microscope. Dated shells were carefully selected within the malacological assemblages according to their abundance to have enough material to be dated from a single sample. In order to avoid the reservoir effect by old carbonate ingestion, the selection of tiny humidity-demanding species (*Vertigo antivertigo*, *Pupilla muscorum*, *Cochlicopa lubrica*) has been favoured (Table 1) (Pigati et al., 2013; Forman et al., 2021; Granai and Wackenheim, 2022). Radiocarbon date of the xerothermic *Cochlicella barbara* shell is consistent with the chronological framework (Wackenheim et al., 2020).

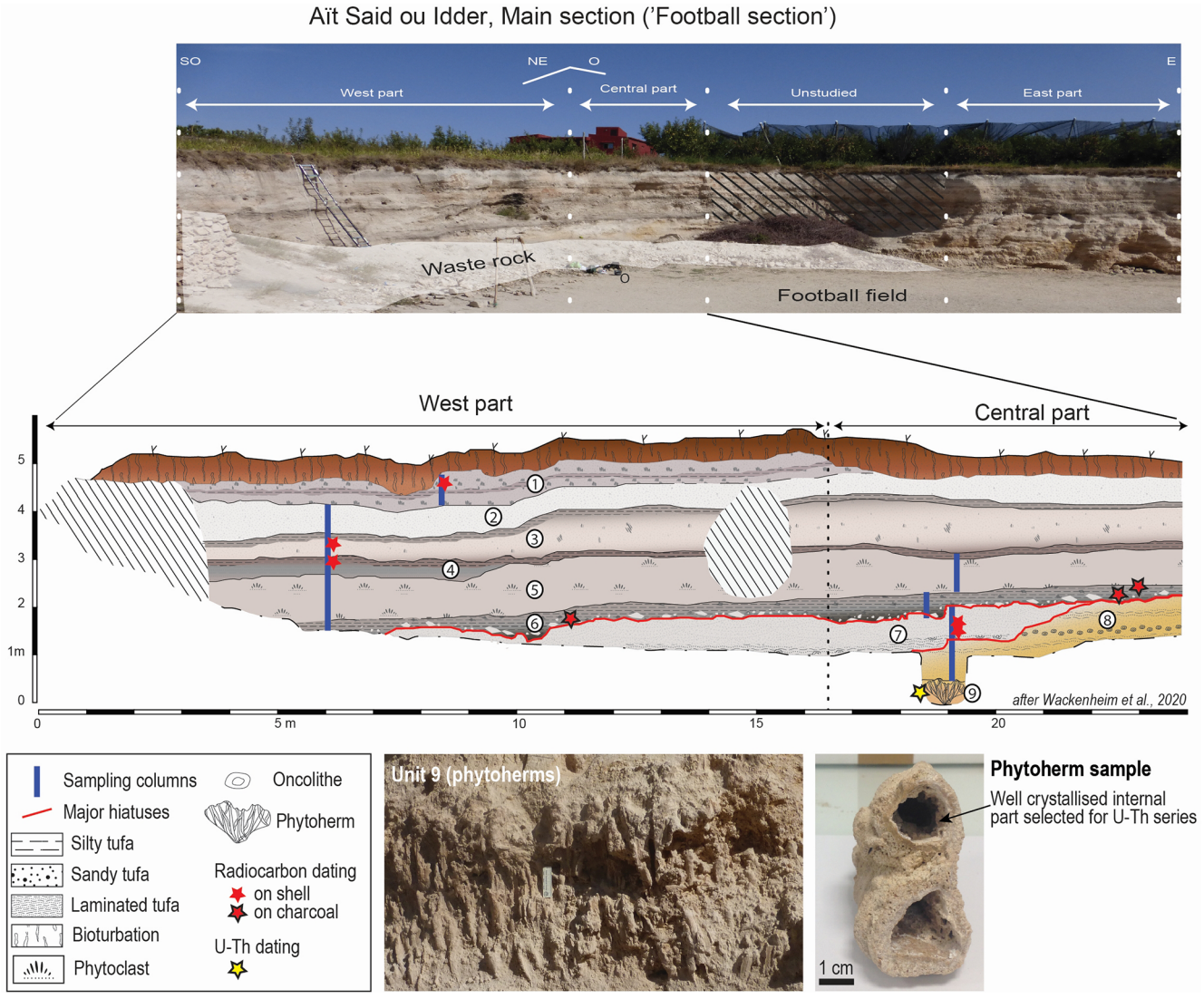

Figure 2. Main section of the Aït Said ou Idder tufa and detailed stratigraphy of the west and central parts where geochemical samples were collected, parallel to malacological samples (modified after Wackenheim et al., 2020). On the bottom right, the picture shows a detailed view of the phytoherm facies from unit 9, which was sampled for the U–Th dating.

Table 1. Details of radiocarbon ages obtained on the Aït Said ou Idder tufa sequence.

Laboratory code	Sample name	Stratigraphic level	Material	^{14}C BP	cal BP 2σ	cal BCE 2σ
Poz-83678	Asi16-Ch	Lower part of grey level D	Charcoal	5830 ± 40	6740–6508	4790–4558
Beta-477595	Asi17-Ch3	Lower part of grey level D	Charcoal	690 ± 30	6553–6405	4604–4456
Beta-477596	Asi17-Ch4	Upper part of grey level D	Charcoal	5470 ± 30	6310–6209	4361–4260
Poz-115941	Asi17-G9	Base unit 5	Charcoal	4730 ± 370	6292–4452	4342–2502
SacA-54562	Asi17-M30	Grey level A	*Vertigo antivertigo*	4375 ± 30	5039–4859	3089–2909
SacA-54563	Asi17-M21	Grey level B	*Cochlicella barbara*	5085 ± 30	5911–5747	3961–3797
SacA-54564	Asi17-M16	Grey level C	*Vertigo antivertigo*	5375 ± 30	6280–6019	4330–4096
DeA-17402	I/1889/1	Unit 7	*Pupilla muscorum*	35 920 ± 530	41 590–39 380	39 640–37 430
DeA-17403	I/1889/2	Unit 7	*Cochlicopa lubrica*	36 720 ± 570	42 170–40 150	40 220–38 200

Radiocarbon dates assigned the upper part of the ASI tufa to the Middle Holocene (from ca. 6800 and 4800 cal BP) while unit 7 from the lower part is dated from the Upper Pleistocene by two coherent dates on land shells (around 37–40 ka cal BP; Table 1 and Fig. 3). To strengthen this chronological framework, we sought an additional date at the base of the tufa deposit. While no suitable organic material or shell was found in units 9 or 10, well-crystallised calcite deposits such as the strongly indurated phytoherms from unit 9 are suitable material for U–Th series analyses (Fig. 2).

3.2 Additional U–Th dating

The U–Th dating method requires well-crystallised calcite samples that are not easily retrieved from tufa deposits dominated by crumbly silty to sandy facies such as those at ASI (Fig. 2); only phytoherms from unit 9 are suitable here for such analyses. One sample selected from unit 9 (Fig. 2) was thus analysed by U series using ICP-Q-MS at the Muséum national d'Histoire naturelle (France). This method relies on the difference in solubility between uranium and thorium. The amount of radiogenic ^{230}Th formed in ratio to its parent ^{234}U yields the age of formation of the calcite (Bourdon et al., 2003; Ivanovich and Harmon, 1992).

The sample was selected in the well-crystallised internal part of the phytoherm cylinder (Fig. 2), cleaned by removing clay and sand adhering on calcite, then cut using a mini rotary tool (Dremel™-like) with a diamond disc, and finally washed with distilled water in an ultrasonic bath. The carbonate (about 0.5 g) was dissolved in HNO_3 acid, and a ^{233}U–^{236}U–^{229}Th mixed spike was added. U and Th chemical extractions and purifications on UTEVA resins were performed according to the protocol detailed by Douville et al. (2010). Each fraction was then dried and dissolved in 2 % $HNHO_3$ before dilution for isotopic analyses by ICP-Q-MS. The measurements were performed on a Thermo iCAP RQ ICP-Q-MS coupled with a Teledyne CETAC Aridus 3 desolvator device. Pre-screening analysis was first performed in order to optimise the final dilutions of each fraction. Then they were combined to be analysed together.

The interface was configured for high sensitivity, and the signal was optimised (tuning) for ^{238}U and ^{235}U on the desolvator and mass spectrometer. The signal intensities of the isotopes ^{229}Th, ^{230}Th, ^{233}U, ^{234}U, ^{235}U and ^{236}U were measured on an electron multiplier (SEM) in pulse-counting mode, and those of ^{232}Th were measured in analogue mode. The helium mode (CCTS) of the collision/reaction cell was used to increase the signal by optimising the ions' focusing. The mass fractionation was corrected by comparing the measured ^{233}U/^{236}U spike ratio with its true known value. The ^{234}U/^{238}U ratio is obtained via the ^{234}U/^{235}U measurement according to the universal natural ^{238}U/^{235}U ratio (Hiess et al., 2012). An analytical standard (without chemistry) of uraninite (HU-1) with a spike, in secular radioactive equilibrium, was analysed along the sequence for machine deviation control. The calculated activity ratios obtained should correspond to the true ratios.

Ages were calculated using half-lives of 75.584 and 245.620 ka for ^{230}Th and ^{234}U, respectively (Cheng et al., 2013). The age uncertainty was estimated taking into account all sources of analytical uncertainty. The U content, isotopic ratios and U-series age of the ASI phytoherm sample are shown in Table 2. The U content is 57 ppb. The ^{234}U/^{238}U is high (more than 3.4) as usually observed in continental carbonates from Morocco (see Ghaleb et al., 2019). An age of 129 ± 4 ka was obtained without correction, but the measured ^{230}Th/^{232}Th ratio of 14 indicates that correction of the age from detritic Th is mandatory. The corrected age, taking into account the average value of the ^{232}Th/^{238}U atomic ratio of the Earth's crust (3.8 ± 2; Ludwig and Paces, 2002), is 123 ± 4 ka and demonstrates the contemporaneity of the bottom of the ASI sequence with Marine Isotopic Stage (MIS) 5e (Fig. 3).

4 Stable isotopes

4.1 Methods

The whole tufa sequence at ASI was sampled continuously every 5 cm (ca. 20 g of tufa was collected for each sample), with local adjustment to stratigraphy when required and excepting the lowermost units 9 and 10, which were too indurated. Each sample was ground when needed and then sifted to < 200 µm to obtain 2 to 5 g of fine material. Stable isotope analyses were performed on CO_2 derived from 40 ± 10 µg of sifted sample, individually reacted with three drops of orthophosphoric acid (H_3PO_4) at 70 °C. Isotope ratios were measured at the Service de Spectrométrie de Masse Isotopique (SSMIM) of the Muséum national d'Histoire naturelle in Paris (France) on a Thermo DELTA V Advantage spectrometer interfaced to a Thermo KIEL IV Carbonate automatic preparation device.

4.2 Results

A summary of ASI isotopic data is given in Table 3, and both δ^{18}O and δ^{13}C are shown in stratigraphic order in Fig. 3. Replicate analyses of the home-made laboratory standard ($n = 29$) gave 2σ precision of 0.1 ‰ for δ^{18}O and 0.08 ‰ for the δ^{13}C. Maximal values, for both δ^{18}O and δ^{13}C, are recorded in samples G81 (−5.3 ‰ and −5.67 ‰, respectively) and G82 (−5.3 ‰ and −6.15 ‰) at the very top of unit 7, below the important sedimentary hiatus with unit 6. These singular values (Fig. 3) are likely to reflect strong diagenetic effects (due to surface alteration and the fire event) and were excluded from the following discussion.

For the remaining samples ($n = 103$), the δ^{18}O values range between −7.8 ‰ and −6.9 ‰ (mean value -7.3 ± 0.1 ‰), whereas δ^{13}C values range between −9.74 ‰ and −7.56 ‰ (mean value -9.25 ± 0.08 ‰; Table 3). Correla-

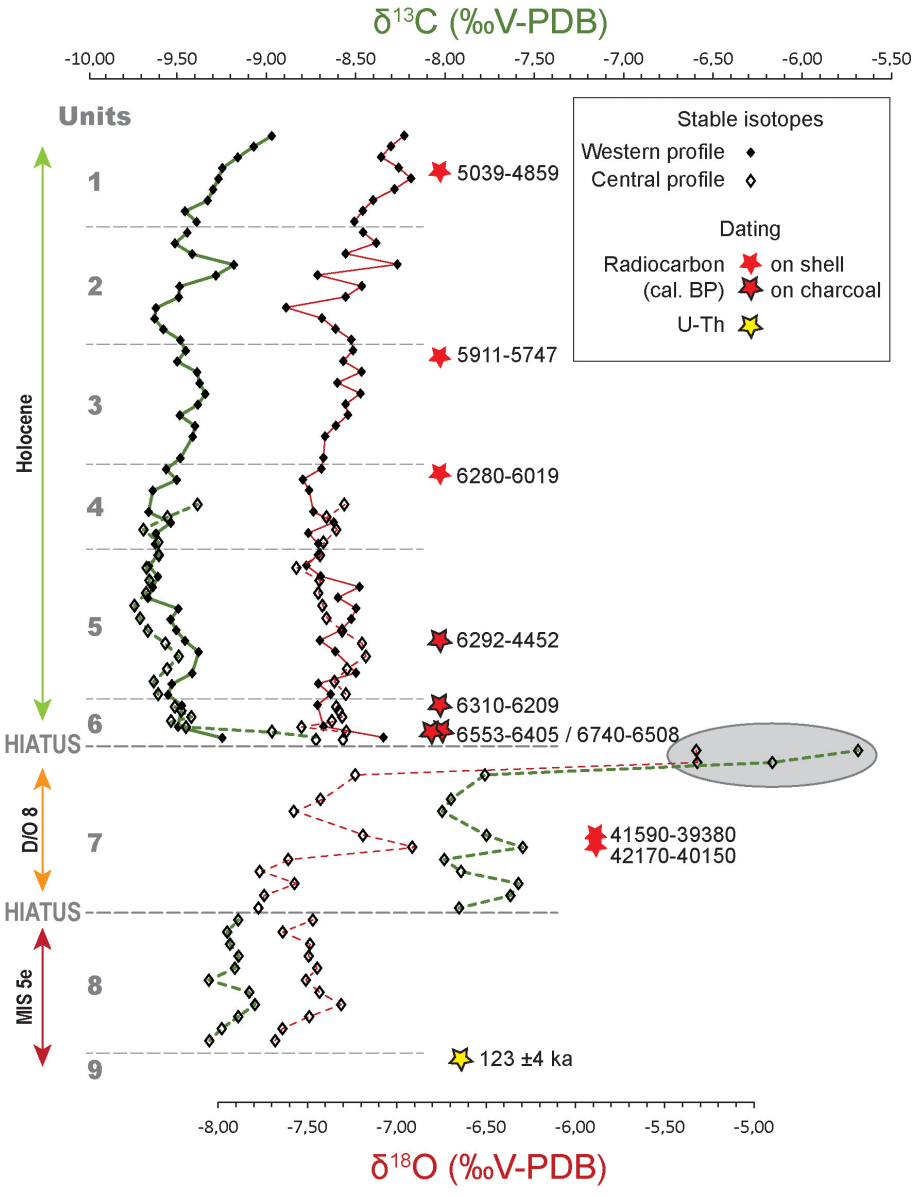

Figure 3. Carbon and oxygen stable isotopes from Aït Said ou Idder tufa calcite shown in stratigraphical order according to tufa units (with no respect to sample depth). The stratigraphical positions of radiocarbon and U–Th ages are also reported.

Table 2. Detailed data from the U series using ICP-Q-MS analyses and resulting age of the phytoherm sample from unit 9 at Aït Said ou Idder.

^{232}Th ppb	± ($k = 2$)	^{234}U/^{238}U	± ($k = 2$)	^{230}Th/^{234}U	± ($k = 2$)	^{230}Th/^{238}U	± ($k = 2$)	^{230}Th/^{232}Th	± ($k = 2$)	Calculated age (ka)	Pos. err.	Neg. err.	Age corr.
29.177	0.488	3.048	0.051	0.771	0.014	2.350	0.042	13.920	0.126	129	4	4	123

Table 3. Summary of stable isotope data from the whole ASI tufa sequence and for the three main phases separated by hiatuses (see text for details).

	$\delta^{18}O$ (‰ V-PDB)	$\delta^{13}C$ (‰ V-PDB)
Conf. int.	0.1	0.08
All, $n = 103$		
Range	−7.8 to −6.9	−9.74 to −7.56
Mean	−7.3	−9.25
SD	0.2	0.57
Upper part, $n = 80$		
Range	−7.6 to −6.9	−9.74 to −8.72
Mean	−7.3	−8.72
SD	0.1	0.18
Unit 7, $n = 12$		
Range	−7.8 to −6.9	−8.01 to −7.56
Mean	−7.4	−7.78
SD	0.3	0.17
Unit 8, $n = 11$		
Range	−7.7 to −7.3	−9.31 to −9.06
Mean	−7.5	−9.18
SD	0.1	0.08

Conf. int.: confidence interval. SD: standard deviation.

tion between $\delta^{18}O$ and $\delta^{13}C$ is not significant ($r = -0.09$; $p = 0.37$; $n = 103$).

At ASI, three phases can be defined, based on sharp variations in the $\delta^{13}C$ at the units 8–7 and then units 7–6 boundaries (Fig. 3 and Table 3): the mean $\delta^{13}C$ value is -9.18 ± 0.08 ‰ ($n = 11$) in the lowermost unit 8, then increases to −7.78 in unit 7 ($n = 12$), and finally decreases suddenly to −9.18 in the rest of the sequence (units 6 to 1; $n = 80$). Boundaries between these three phases are correlated to main hiatuses observed in the stratigraphic sequence of ASI (Fig. 2). Conversely, the $\delta^{18}O$ remains stable from part to part (−7.5 ‰, −7.4 ‰ and -7.3 ± 0.1 ‰, respectively; Table 3). Within each phase, variations in both $\delta^{13}C$ and $\delta^{18}O$ are low (standard variations equal or close to confidence intervals; Table 3). According to stratigraphy and dating, these phases correspond to three distinct periods of time separated by hiatuses: from bottom to top, units 9 and 8 are assigned to the early MIS 5e, unit 7 is dated to around 37–40 ka cal BP (during MIS 3), and units 6 to 1 record part of the Middle Holocene (Fig. 3).

5 Discussion

5.1 ASI tufa chronology compared to other regional tufas and its climatic significance

In Morocco, Late Pleistocene tufa deposits are reported during both odd and even Marine Isotopic Stages (MISs) (Rousseau et al., 2017; Weisrock et al., 2008), i.e. during interglacial and glacial periods (Fig. 4). Over the last 130 kyr, at the northern border of the Moroccan Sahara, Weisrock et al. (2008) showed (based on U–Th dating) that most tufas were deposited during MIS 5, then between 50–30 and 24–11 ka (Figs. 1 and 4). In detail, at least two main phases of deposition occurred during MIS 5, at 120–130 ka (i.e. during MIS 5e) and 90–74 ka (Fig. 4; Boudad et al., 2003; Falguères et al., 2016; Weisrock et al., 2008). Few Holocene tufas have been reported in Morocco so far, except in the Ksabi basin (e.g. at Blirh and Aït Blal; Lefèvre, 1989; Limondin-Lozouet et al., 2013; Vaudour, 1986) and the Aïn Beni Mathar basin (Depreux et al., 2021; Wengler and Vernet, 1992), in the Moulouya catchment, where they are dated from the Early Holocene (Figs. 1 and 4). Later tufa deposits were recently dated from the last 5000 years at Imouzzer Kandar (Azennoud et al., 2022), only a few kilometres from ASI (Figs. 1 and 4).

On the other side of the Strait of Gibraltar, Spanish tufa deposits have been more extensively studied for decades and regional synthesis are available (see González Martín and González Amuchastegui, 2014). Many tufa or travertine deposits have thus been reported in Andalusia, mostly supporting geomorphological and sedimentological investigations (Durán, 1996; García-García et al., 2014; Martìn-Algarra et al., 2003; Pla-Pueyo et al., 2017; Prado-Pérez et al., 2013). From a climatic point of view, northeastern Morocco and Andalusia nowadays present strong similarities as they both experience Mediterranean conditions with hot summers and low-pressure westerlies bringing air masses from the Atlantic which result in mean annual precipitation in excess of 100 to 250 mm yr^{-1} during winters and springs (Larrasoaña et al., 2013; Lionello, 2012; New et al., 2000). It thus seems relevant in order to expand the corpus of comparison sites to include data from Andalusia where five phases of maximal tufa deposition have been identified since 130 ka (Delgado Castilla, 2007; Durán, 1996; Martìn-Algarra et al., 2003), including both MIS 1 and MIS 5 interglacials but also the MIS 2–MIS 1 transition and two phases during the Last Glacial Period at around 20–25 ka (MIS 2) and around 40 ka (MIS 3; Fig. 4).

Pleistocene deposits observed at ASI during the early MIS 5e, then around 37–40 ka cal BP, are thus contemporaneous with phases of maximal tufa deposition observed in both Spain and Morocco (Fig. 4). The youngest phase of maximal tufa deposition at ASI has only been faintly observed in Morocco, where only a few well-dated Holocene tufa deposits

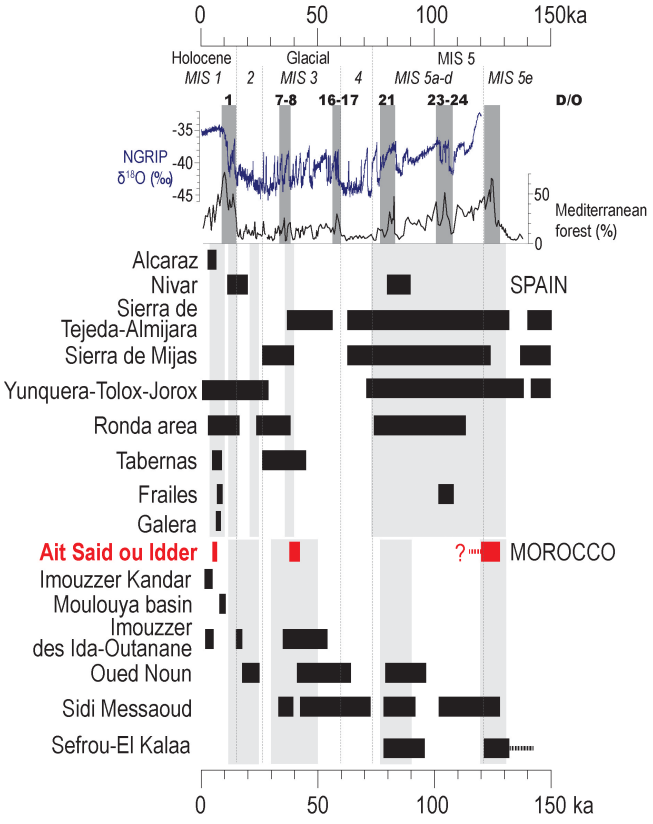

Figure 4. Chronological distribution of tufa deposits from southern Spain (Andrews et al., 2000; Delannoy et al., 1993; Delgado Castilla, 2009; Durán, 1996; García-García et al., 2014; Martìn-Algarra et al., 2003; Wolf et al., 2021) and from Morocco (Azennoud et al., 2022; Boudad et al., 2003; Depreux et al., 2021; Falguères et al., 2016; Lefèvre, 1989; Mercier et al., 2009; Rousseau et al., 2006; Weisrock et al., 2008) including ASI (this study, in red) compared to the evolution of Greenland δ^{18}O (North Greenland Ice Core Project members, 2004) and Mediterranean forest at the SW Iberian margin (MD95-2042; Sánchez Goñi et al., 2008) during the last climatic cycle. MIS: Marine Isotopic Stage. D/O: Dansgaard–Oeschger events (in bold). Darker grey bars highlight the main developments of the Mediterranean forest (associated with precession minima and high atmospheric methane concentrations, after Sánchez Goñi et al., 2008). Lighter grey bars highlight maxima in tufa depositions in Spain (Durán, 1996) and in northern Morocco (Rousseau et al., 2006; Weisrock et al., 2008). Localisation of sites is shown in Fig. 1.

have been reported (in the Moulouya basin), but has been well identified in Spain (Fig. 4).

Under European mid-latitudes, tufa deposits are usually associated with interglacial conditions (Pentecost, 1993, 1995), but some examples show that they can rapidly develop as soon as climatic conditions improve and before the establishment of trees in the deglaciated landscape. Less is known about tufas in sub-tropical areas (Ford and Pedley, 1996), but they are usually considered records of humid (pluvial) phases (Butzer et al., 1978; Delgado Castilla, 2009; Hamdan and Brook, 2015; Nicod, 2000).

As recorded by maxima of the Mediterranean forest in marine cores from the SW Iberian margin and the Alboran Sea, the Mediterranean climate (characterised by warm and dry summers and especially humid winters) appears well expressed during interglacials (MIS 1 and MIS 5e); MIS 5 interstadials; and D–O interstadials 16–17, 8 and 7 (Combourieu-Nebout et al., 2002; Fletcher and Sánchez Goñi, 2008; Sánchez Goñi et al., 2008, 2000). Specifically, D–O event 8 corresponds to one of the longest and wettest interstadials recorded in the western Mediterranean during the glacial period (Combourieu-Nebout et al., 2002; Margari et al., 2010; Sánchez Goñi et al., 2008).

Phases of maximal tufa deposition observed in Morocco and southern Spain thus appear contemporaneous with these periods of maximal development of the Mediterranean forest, which confirms that their chronological distribution is mainly driven by climatic parameters (Delgado Castilla, 2007; Rousseau et al., 2006; Weisrock et al., 2008). At ASI, tufa deposits are reported during periods when Mediterranean climatic conditions, especially winter humidity, were particularly marked, i.e. during the Holocene, the Eemian, and D–O interglacial 8 (Sánchez Goñi et al., 2008; Shackleton et al., 2004; Zielhofer et al., 2017; Fig. 4).

5.2 Comparison of intensities of the Holocene and Eemian interglacials and D–O interstadial 8 at Aït Said ou Idder

Climatic parameters influencing stable isotopes in modern and Quaternary tufa deposits have been well identified (Andrews, 2006; Andrews et al., 1997; Dabkowski et al., 2011). Tufa calcite δ^{18}O is directly linked to local air mass composition, which mainly depends on their source, rainout effects due to "continentality", altitude or processes such as the amount effect, and changes in the atmospheric temperature. On the other hand, tufa calcite δ^{13}C is influenced by biomass type and abundance and rainfall amount (i.e. moisture availability).

The three chronological phases identified at ASI are characterised by different isotopic signatures: regarding the δ^{13}C, sedimentary hiatuses between those phases correspond to shifts in the carbon isotope composition of tufa, while the δ^{18}O shows smaller variations (Fig. 3). This remarkable homogeneity of δ^{18}O values (Table 3) suggests no significant difference in terms of temperature or air mass circulation between the Holocene, D–O interstadial 8 and MIS 5e. Regarding carbon isotopes, D–O 8 records values close to −8 ‰ (Table 3), significantly higher than during the interglacials, which reflect a lesser development of soil and vegetation under relatively "drier" conditions during this MIS 3 interstadials (Fig. 5). On the other hand, both interglacials present δ^{13}C values typical of a strong influence from C_3 plant-/soil-zone CO_2 in δ^{13}C (Andrews, 2006; Fig. 5), suggesting rela-

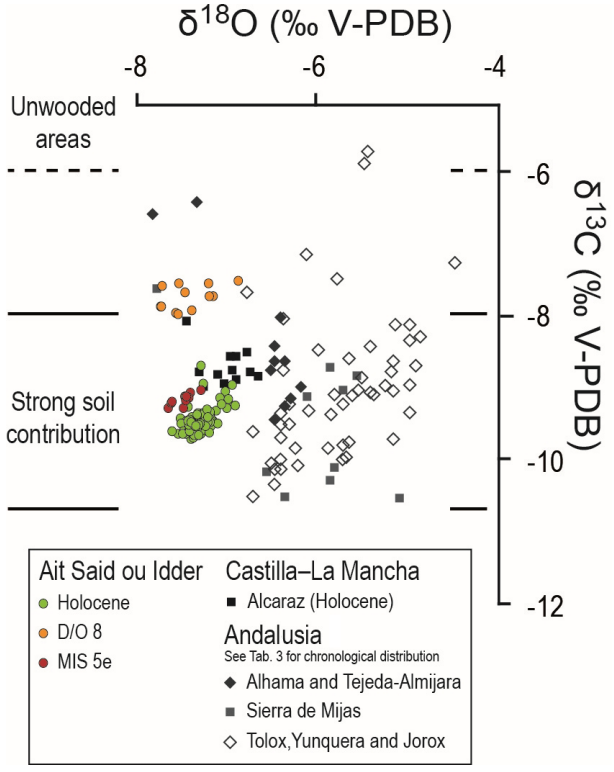

Figure 5. Combined δ^{18}O and δ^{13}C plot for Aït Said ou Idder compared to isotopic data available from some southern Spain tufa deposits. The three phases of tufa depositions are shown for ASI data, but detailed chronological attribution is not available for Andalusian tufa deposits (Table 4): at Frailes, two phases of tufa deposits are dated from the Holocene and from MIS 5, respectively (see Fig. 4), and seven unassigned samples were analysed for isotopes (García-García et al., 2014; Pla-Pueyo et al., 2017); other Andalusian tufa deposits are dated from the Late and Middle Pleistocene with only two samples assigned to the Holocene at Jorox (Durán, 1996). All Alcaraz data (Castilla–La Mancha) are from the Holocene (Andrews et al., 2000). Ranges of carbon isotopic values related to sites where soils are well developed or, conversely, unwooded areas are according to Andrews (2006) and Andrews et al. (1997).

tively wet conditions. The narrower range of carbon isotope variations recorded during MIS 5e at ASI may result from a lower number of samples for the period ($n = 11$) compared to the Holocene ($n = 80$; Table 3); however, considering means and standard deviations, MIS 5e seems to record higher δ^{13}C values, suggesting slightly reduced moisture with regard to the Holocene (Table 3).

These observations are consistent with the environmental reconstructions provided by malacological investigations on the very same profile at ASI (Wackenheim et al., 2020): mollusc assemblages assigned to D–O 8 (i.e. from unit 7) suggest a more open environment under drier conditions than during the Holocene (from units 6 to 1). In the units assigned to MIS 5e, shells are fewer but may suggest wet conditions, similar to those observed during the Holocene.

Palaeoclimatic reconstructions obtained from a transfer function technique on fossil pollen assemblages from marine cores from west and east Iberia (MD95-2042 and ODP 976; Fig. 1) suggest that temperature conditions during MIS 3 interstadials were similar to present-day (Holocene) values (Sánchez Goñi et al., 2002) as also suggested by the ASI δ^{18}O record. Estimated annual rainfall is less reliable due to methodological limits. Nevertheless, the transfer function reconstructs annual precipitation that is similar during D–O 8 and MIS 1 on both sides of Iberia (Sánchez Goñi et al., 2002). However, MIS 3 interstadials, including D–O 8, are millennial-scale events during which the development of temperate and Mediterranean forests remained reduced with respect to the MIS 1 and MIS 5e interglacials (Camuera et al., 2019; Combourieu-Nebout et al., 2002; Sánchez Goñi et al., 2000; Fig. 4). As the moisture signal recorded by tufa δ^{13}C partly depends on the biomass abundance, the higher carbon isotopic values observed at ASI during D–O 8 could reflect the lesser development of the forest cover while the rainfall amount and other moisture factors are consistent with those from interglacial periods.

Comparing the Holocene and MIS 5e interglacials, a compilation of continental and marine palaeoenvironmental records from North Africa and the surrounding areas suggests that mean annual precipitation in Mediterranean Africa, including northern Morocco, was higher than in the present day at both 6–10 and 122–128 ka cal BP (up to 1000 mm yr^{-1}, while present-day mean annual precipitation is $\leq$ 500 mm yr^{-1}) (Larrasoaña et al., 2013). At the regional scale, the palynological data from a long core from the Padul wetland (Andalusia) suggest warmer and/or wetter conditions during the last interglacial compared to the Holocene (Camuera et al., 2019), as in other pollen records from the Mediterranean regions (e.g. Djamali et al., 2008; Litt et al., 2014; Tzedakis and Bennett, 1995). In detail, these different climates may result from strong differences in seasonality: explicitly more marked summer droughts but higher winter precipitation during the last interglacial (Camuera et al., 2019).

The growth of tufa deposits is by nature linked to water availability (Pentecost, 2005); tufa deposition is thus likely to be reduced during dry summers but favoured by autumn/winter rainfall. However, δ^{13}C data from ASI are not consistent with those observations as they rather suggest no difference or even slightly drier conditions during MIS 5e compared to the Holocene. We notice that such strong MIS 5e seasonality may also affect the δ^{18}O signal through the "amount effect" (concentration of precipitation during the wet/cool season) and the seasonal growth of tufa deposition, both of which would lead to the selective record of winter (cool) temperature conditions. In this case, the record of warmer (summer) MIS 5e conditions (as observed in the Padul record) in ASI δ^{18}O would be dampened.

5.3 Comparison with Spanish data

Isotopic data are also available from some tufa deposits from southern Spain (Figs. 1 and 5). The Alcaraz tufa deposits in Castilla–La Mancha have been clearly assigned to the Middle Holocene based on pollen and mollusc data and on two radiocarbon dates (Andrews et al., 2000). At least part of the Alcaraz deposits is contemporaneous with those from ASI (Fig. 4).

Unfortunately, the chronological attribution of the isotopic data available in Andalusia is less precise: the authors provide a chronology based on U–Th dating of several phases of tufa development in the area (Fig. 4) but have not clearly discriminated the geochemical samples according to those phases (Durán, 1996; García-García et al., 2014); i.e. each sample cannot be specifically assigned to a period. Data from Andalusian tufas shown in Fig. 5 are dated from the Late and Middle Pleistocene (Table 4), mostly from MIS 5 except in the Tolox–Yunquera–Jorox area, where more than half of the samples are older than 300 ka (Table 4). Only two samples, at Jorox, are assigned to the Holocene (Durán, 1996). At Frailes, tufa developed during MIS 5 (around 100–110 ka) and then during the Early Holocene, but the specific chronological attribution of the seven samples analysed at this site is not given (García-García et al., 2014; Pla-Pueyo et al., 2017).

As at ASI, most $\delta^{13}C$ values from southern Spain range between ca. $-10\,‰$ and $-8\,‰$, whatever their age, which demonstrates a strong influence from C_3 plant-/soil-zone CO_2 (Andrews, 2006; Fig. 5) and suggests relatively wet conditions. Carbon isotope values from Frailes are higher (up to $-6.35\,‰$; Pla-Pueyo et al., 2017) but remain close to those prevailing at ASI during D–O 8, never reaching values typical of unwooded areas (Fig. 5). On both sides of the western Mediterranean, there is thus no evidence of strong aridity that would have led to evaporation processes and less negative $\delta^{13}C$ values in tufa (Andrews, 2006). This is strongly consistent with the prior assumption that, in pluvial and subtropical areas, tufa deposits are observed during humid (interglacial or interstadial) phases (Butzer et al., 1978; Delgado Castilla, 2009; Depreux et al., 2021; Hamdan and Brook, 2015; Nicod, 2000).

Regarding $\delta^{18}O$ values, larger variations are observed. Alcaraz (Holocene) oxygen data are roughly similar to those from ASI (typically between $-7.5\,‰$ and $-6.7\,‰$; Andrews et al., 2000). At Frailes, $\delta^{18}O$ values remain close to those from ASI (ranging from $-6.70\,‰$ to $-5.67\,‰$; Pla-Pueyo et al., 2017), but those from Pleistocene Andalusian tufa deposits studied by Durán (1996) are significantly higher, whatever their age (Fig. 5). In the Tolox–Yunquera–Jorox area, where a majority of analysed samples are older than 300 ka (Table 4), $\delta^{18}O$ values are the highest and reach up to $-4.2\,‰$ (Fig. 5; Durán, 1996).

Using the Online Isotopes in Precipitation Calculator (OIPC; Bowen, 2022; Bowen and Revenaugh, 2003; IAEA/WMO, 2015), extrapolations of the mean annual $\delta^{18}O$ for modern precipitation are $-7.8 \pm 0.2\,‰$ at ASI, $-8.1 \pm 0.3\,‰$ at Alcaraz and $-7.2 \pm 0.3\,‰$ at Frailes, and they range between ca. $-6\,‰$ and $-5.5\,‰$ at other Andalusian sites. The rainfall water $\delta^{18}O$ values are thus similar at ASI, Frailes and Alcaraz but are up to $3\,‰$ higher at Andalusian sites studied by Durán (1996), the same amplitudes as observed in tufa $\delta^{18}O$ (Fig. 5).

ASI, Frailes and Alcaraz are all at relatively high altitude (> 975 m a.s.l.), while the other tufa deposits studied in Andalusia are below 500 m a.s.l. Tufa $\delta^{18}O$ values decreasing with altitude have been similarly observed at Alpine sites; the combined effects of the progressive rainout of air mass and condensation of water at high altitude result in lower rainfall $\delta^{18}O$ (Andrews et al., 1997). Consequently, the lower $\delta^{18}O$ values observed at ASI, Frailes and Alcaraz are likely to reflect orogenic effects. Furthermore, with the lack of precise chronological attribution of $\delta^{18}O$ data from Andalusia, whether or not Pleistocene interglacials were warmer compared to the Holocene in Spain cannot be solved, in contrast with Morocco where a remarkable consistency is recorded at ASI between MIS 5, D–O 8 and the Holocene.

6 Conclusion and further remarks

Tufa chronological distribution in the southwestern Mediterranean area is mainly driven by climatic parameters: tufas are characteristic of humid (interglacial or interstadial) phases. At Aït Said ou Idder and more generally in both Morocco and southern Spain, phases of maximal tufa deposition appear indeed contemporaneously with periods of maximal development of the Mediterranean forest. Additionally, ASI $\delta^{13}C$ values show no evidence of evaporation processes that may result from strong aridity, which is similarly observed in tufa deposits from Andalusia. However, we may notice that no tufa deposit is reported during D–O 16–17, neither in Morocco nor in southern Spain, while one of the strongest developments of the Mediterranean forest is recorded during this event (Fig. 4). This questions the relationship between tufa deposits and both the duration and the seasonality of humid periods: some humid events might be too short to allow the onset of tufa deposition, and/or contrasting seasons are not favourable to it.

No significant difference in terms of temperature or air mass circulation is observed in the Middle Atlas between the Holocene, D–O interstadial 8 and MIS 5e, according to ASI oxygen stable isotopes. Regarding moisture conditions, D–O 8 is marked by a lesser development of soil and vegetation as conditions were drier than during MIS 1 and MIS 5e. During both these interglacials, wet conditions are recorded according to ASI $\delta^{13}C$, but MIS 5e could be slightly less wet than the Holocene. However, comparisons with regional (marine and continental) climatic records suggest that this observation might actually reflect stronger seasonality during MIS 5e. Such diachronic comparison cannot be extended

Table 4. Number of samples analysed for stable isotopes in Andalusia and their chronological distribution according to Durán (1996), García-García et al. (2014) and Pla-Pueyo et al. (2017).

	> 300 ka	MIS 7	MIS 5	MIS 3	MIS 2	MIS 1	Total samples
Alhama and Tejeda–Almijara		5	6	2			13
Sierra des Mijas	1	4	5		2		12
Tolox, Yunquera and Jorox	32		18		1	2	53
Frailes			?			?	7
Total	33	9	≥ 29	2	3	≥ 2	85

to Morocco and southern Spain yet, nor can comparison between both sides of the Strait of Gibraltar be made because of the lack of well-dated isotopic data from tufa deposits in the area.

Our preliminary investigations thus demonstrate that calcareous tufa deposits have strong potential to feed discussions on climate variability, at different scales of space and time, in the southeastern Mediterranean area where they appear to be well represented. However, new dates and new isotopic data are required from both already known sites and newly investigated sequences.

Data availability. Full data are available on request to Julie Dabkowski (julie.dabkowski@lgp.cnrs.fr).

Sample availability. Tufa samples are available on request to Julie Dabkowski (julie.dabkowski@lgp.cnrs.fr).

Author contributions. JD, QW, NLL and LB conducted the fieldwork, with contributions from JFB. QW performed the malacological analyses under the supervision of NLL and provided selected material for radiocarbon dating on shells. CF and OT performed the U–Th series analyses on calcite. DF ran the isotopic analyses at the SSMIM (MNHN, Paris) and provided support to JD in terms of data discussion. The manuscript was written by JD with contributions from all the co-authors.

Competing interests. The contact author has declared that neither they nor their co-authors have any competing interests.

Disclaimer. Publisher's note: Copernicus Publications remains neutral with regard to jurisdictional claims in published maps and institutional affiliations.

Acknowledgements. The authors thank both reviewers for their kind and constructive comments on the manuscript.

Financial support. Fieldwork and analyses at Aït Said ou Idder were mostly funded by the PALEOMEX (INSU–INEE) Transect Maghreb research programme (Jean-François Berger). Radiocarbon ages have been supported by the LMC14 (CEA, Gif-sur-Yvette) Artemis programme and by the Czech Science Foundation (grant no. P504/17-05696S).

Review statement. This paper was edited by Becky Briant and reviewed by Jonathan Holmes and Philip Hopley.

References

Andrews, J. E.: Palaeoclimatic records from stable isotopes in riverine tufas: Synthesis and review, Earth-Sci. Rev., 75, 85–104, https://doi.org/10.1016/j.earscirev.2005.08.002, 2006.

Andrews, J. E., Riding, R., and Dennis, P. F.: The stable isotope record of environmental and climatic signals in modern terrestrial microbial carbonates from Europe, Palaeogeogr. Palaeocl., 129, 171–189, https://doi.org/10.1016/S0031-0182(96)00120-4, 1997.

Andrews, J. E., Pedley, M., and Dennis, P. F.: Palaeoenvironmental records in Holocene Spanish tufas: a stable isotope approach in search of reliable climatic archives, Sedimentology, 47, 961–978, 2000.

Azennoud, K., Baali, A., Ait Brahim, Y., Ahouach, Y., and Hakam, O.: Climate controls on tufa deposition over the last 5000 years: A case study from Northwest Africa, Palaeogeogr. Palaeocl., 586, 110767, https://doi.org/10.1016/j.palaeo.2021.110767, 2022.

Boudad, L., Kabiri, L., Farkh, S., Falguères, C., Rousseau, L., Beauchamp, J., Nicot, É., and Cairanne, G.: Datation par la méthode U/Th d'un travertin quaternaire du Sud-Est marocain: implications paléoclimatiques pendant le Pléistocène moyen et supérieur, C. R. Geosci., 335, 469–478, https://doi.org/10.1016/S1631-0713(03)00081-6, 2003 (in French with abridged English version).

Bourdon, B., Henderson, G. M., Lundstrom, C. C., and Turner, S.: U-series geochemistry, Rev. Mineral. Geochem., 52, 1–656, 2003.

Bowen, G. J.: The Online Isotopes in Precipitation Calculator, version 3.1, https://wateriso.utah.edu/waterisotopes/pages/data_access/oipc_citation.html, last access: 22 February 2022.

Bowen, G. J. and Revenaugh, J.: Interpolating the isotopic composition of modern meteoric precipitation: isotopic composi-

tion of modern precipitation, Water Resour. Res., 39, 1299, https://doi.org/10.1029/2003WR002086, 2003.

Butzer, K. W., Stuckenrath, R., Bruzewicz, A. J., and Helgren, D. M.: Late Cenozoic Paleoclimates of the Gaap Escarpment, Kalahari margin, South Africa, Quaternaty Res., 10, 310–339, https://doi.org/10.1016/0033-5894(78)90025-X, 1978.

Camuera, J., Jiménez-Moreno, G., Ramos-Román, M. J., García-Alix, A., Toney, J. L., Anderson, R. S., Jiménez-Espejo, F., Bright, J., Webster, C., Yanes, Y., and Carrión, J. S.: Vegetation and climate changes during the last two glacial-interglacial cycles in the western Mediterranean: A new long pollen record from Padul (southern Iberian Peninsula), Quaternary Sci. Rev., 205, 86–105, https://doi.org/10.1016/j.quascirev.2018.12.013, 2019.

Capezzuoli, E., Gandin, A., and Pedley, M.: Decoding tufa and travertin (fresh water carbonates) in the sedimentary record: The state of the art, Sedimentology, 61, 1–21, https://doi.org/10.1111/sed.12075, 2014.

Cheng, H., Edward, R. L., Shen, C.-C., Polyak, V. J., Asmerom, Y., Woodhead, J. , Hellstrom, J., Wang, Y., Kong, X. , Spötl, C., Wang X., and Alexander Jr., E. C.: Improvements in 230Th dating, ^{230}Th and ^{234}U half-life values, and U–Th isotopic measurements by multi-collector inductively coupled plasma mass spectrometry, Earth Planet. Sc. Lett., 371–372, 82–91, https://doi.org/10.1016/j.epsl.2013.04.006, 2013.

Combourieu-Nebout, N. C., Turon, J. L., Zahn, R., Capotondi, L., Londeix, L., and Pahnke, K.: Enhanced aridity and atmospheric high-pressure stability over the western Mediterranean during the North Atlantic cold events of the past 50 k.y., Geology, 30, 863–866, https://doi.org/10.1130/0091-7613(2002)030<0863:EAAAHP>2.0.CO;2, 2002.

Dabkowski, J.: High potential of calcareous tufas for integrative multidisciplinary studies and prospects for archaeology in Europe, J. Archaeol. Sci., 52, 72–83, https://doi.org/10.1016/j.jas.2014.07.013, 2014.

Dabkowski, J.: The late-Holocene tufa decline in Europe: Myth or reality?, Quaternary Sci. Rev., 230, 106141, https://doi.org/10.1016/j.quascirev.2019.106141, 2020.

Dabkowski, J. and Limondin-Lozouet, N.: Intensities (temperature and humidity) of MIS 11 and MIS 5e interglacials compared to the Holocene using stable isotopes from Northern France (Paris Basin) tufa deposits, Quaternary Res., 1–2, https://doi.org/10.1017/qua.2021.66, 2021.

Dabkowski, J., Limondin-Lozouet, N., Antoine, P., Marca-Bell, A., and Andrews, J.: Enregistrement des variations climatiques au cours des interglaciaires d'après l'étude des isotopes stables de la calcite de tufs calcaires pléistocénes du nord de la France : exemple des séquences de Caours (SIM 5e ; Somme) et de La Celle-sur-Seine (SIM 11; Seine-et-Marne), Quaternaire, 22, 275–283, https://doi.org/10.4000/quaternaire.6010, 2011 (in French).

Delannoy, J.-J., Guendon, J.-L., Quinif, Y., and Roiron, P.: Formaciones travertínicas del piedemonte mediterráneo de la Serranía de Ronda (Málaga), Cuadernos de geografía, 54, 189–222, 1993 (in Spanish).

Delgado Castilla, L.: Edades U/Th de los travertinos del cuaternario reciente de la cuenca de Tabernas, Almeria (SE de España) y sus implicaciones en la evolucion geodinámica y paleoambiental de esta, in: Contribuciones al Estudio del Periodo Cuaternario – Resúmenes XII Reunión Nacional de Cuaternario, edited by: Lario, J. and Silva, P. G., Aequa, Ávila, Spain, 45–46, 2007 (in Spanish).

Delgado Castilla, L.: Edades U/Th de los travertinos del cuaternario reciente de la cuenca de Tabernas, Almería: implicaciones en su evolución geodinámica y paleoambiental, Revista Cuaternario y Geomorfología, 23, 65–76, 2009 (in Spanish).

Depreux, B., Lefèvre, D., Berger, J.-F., Segaoui, F., Boudad, L., El Harradji, A., Degeai, J.-P., and Limondon-Lozouet, N.: Alluvial records of the African Humid Period from the NW African highlands (Moulouya basin, NE Morocco), Quaternary Sci. Rev., 255, 106807, https://doi.org/10.1016/j.quascirev.2021.106807, 2021.

Djamali, M., de Beaulieu, J.-L., Shah-hosseini, M., Andrieu-Ponel, V., Ponel, P., Amini, A., Akhani, H., Leroy, S. A. G., Stevens, L., Lahijani, H., and Brewer, S.: A late Pleistocene long pollen record from Lake Urmia, NW Iran, Quaternary Res., 69, 413–420, https://doi.org/10.1016/j.yqres.2008.03.004, 2008.

Douville, E., Sallé, E., Frank, N., Eisele, M., Pons-Branchu, E., and Ayrault, S.: Rapid and accurate U–Th dating of ancient carbonates using inductively coupled plasma-quadrupole mass spectrometry, Chem. Geol., 272, 1–11, https://doi.org/10.1016/j.chemgeo.2010.01.007, 2010.

Durán, J. J.: Los sistemas kársticos de la provincia de Málaga y su evolución: Contribución al conocimiento paleoclimático del Cuaternario en el Mediterráneo occidental, PhD thesis, Complutense University of Madrid, Spain, 409 pp., 1996 (in Spanish).

Falguères, C., Weisrock, A., Ghaleb, B., Haddad, M., Janati-Idrissi, N., Bejjit, L., Gourari, L., Rousseau, L., Boudad, L., Taous, A., Beauchamp, J., and Pozzi, J.-P.: Datations par les series de l'uranium et par ESR des travertins du Pleistocene superieur (MIS5) de Sefrou-El Kalaa (Maroc) et leurs implications paleoenvironnementales, in: Actes de la Septième Rencontre des Quaternaristes Marocains (RQM7), Quaternaire du Nord-Ouest de l'Afrique, Agadir, Maroc, 273–281, ISBN: 978-9954-0-5399-7, 2016 (in French).

Fletcher, W. J. and Sánchez Goñi, M. F.: Orbital- and sub-orbital-scale climate impacts on vegetation of the western Mediterranean basin over the last 48,000 yr, Quaternary Res., 70, 451–464, https://doi.org/10.1016/j.yqres.2008.07.002, 2008.

Ford, T. D. and Pedley, H. M.: A review of tufa and travertine deposits of the world, Earth-Sci. Rev., 41, 117–175, https://doi.org/10.1016/S0012-8252(96)00030-X, 1996.

Forman, S. L., Hockaday, W., Liang, P., and Ramsey, A.: Radiocarbon age offsets, ontogenetic effects, and potential old carbon contributions from soil organic matter for pre-bomb and modern detritivorous gastropods from central Texas, USA, Palaeogeogr. Palaeocl., 583, 110671, https://doi.org/10.1016/j.palaeo.2021.110671, 2021.

García-García, F., Pla-Pueyo, S., Nieto, L. M., and Viseras, C.: Sedimentology of geomorphologically controlled Quaternary tufas in a valley in southern Spain, Facies, 60, 53–72, https://doi.org/10.1007/s10347-013-0361-5, 2014.

Ghaleb, B., Falguères, C., Carlut, J., Pozzi, J. P., Mahieux, G., Boudad, L., and Rousseau, L.: Timing of the Brunhes-Matuyama transition constrained by U-series disequilibrium, Sci. Rep.-UK, 9, 6039, https://doi.org/10.1038/s41598-019-42567-2, 2019.

González Martín, J. A. and González Amuchastegui, M. J. (Eds.): Las Tobas en España, SEG, Badajoz, ISBN: 978-84-697-1469-0, 2014 (in Spanish).

Goudie, A. S., Viles, H. A., and Pentecost, A.: The late-Holocene tufa decline in Europe, The Holocene, 3, 181–186, 1993.

Granai, S. and Wackenheim, Q.: La datation radiocarbone sur coquilles de mollusques continentaux: quelles limites et quels usages?, in: Mesurer le temps de l'âge du Bronze, Actes de la journée thématique de l'APRAB, Saint-Germain-en-Laye, France, 21–33, 2022 (in French).

Hamdan, M. A. and Brook, G. A.: Timing and characteristics of Late Pleistocene and Holocene wetter periods in the Eastern Desert and Sinai of Egypt, based on ^{14}C dating and stable isotope analysis of spring tufa deposits, Quaternary Sci. Rev., 130, 168–188, https://doi.org/10.1016/j.quascirev.2015.09.011, 2015.

Hiess, J., Condon, D., McLean, N., and Noble, S. R.: $^{238}U/^{235}U$ systematics in terrestrial uranium-bearing minerals, Science, 335, 1610–1614, https://doi.org/10.1126/science.1215507, 2012.

Ivanovich, M. and Harmon, R. S.: Uranium-series Disequilibrium: Applications to Earth, Marine and Environmental Sciences, 2nd edn., Clarendon Press, Oxford, ISBN 978-1-4020-4496-0, 1992.

Larrasoaña, J. C., Roberts, A. P., and Rohling, E. J.: Dynamics of Green Sahara Periods and Their Role in Hominin Evolution, PLoS ONE, 8, e76514, https://doi.org/10.1371/journal.pone.0076514, 2013.

Lefèvre, D.: Formations continentales pléistocenes et paléoenvironnements sédimentaires dans le bassin de Ksabi (Moyenne Moulouya, Maroc), Bulletin de l'Association française pour l'étude du quaternaire, 26, 101–113, https://doi.org/10.3406/quate.1989.1897, 1989 (in French).

Limondin-Lozouet, N.: Successions malacologiques à la charnière Glaciaire/Interglaciaire: du modèle Tardiglaciaire-Holocène aux transitions du Pleistocène, Quaternaire, 22, 211–220, 2011 (in French).

Limondin-Lozouet, N. and Preece, R. C.: Quaternary perspectives on the diversity of land snail assemblages from northwestern Europe, J. Molluscan Stud., 80, 224–237, https://doi.org/10.1093/mollus/eyu047, 2014.

Limondin-Lozouet, N., Haddoumi, H., Lefèvre, D., Ghamizi, M., Aouraghe, H., and Salel, T.: Holocene molluscan succession from NE Morocco: Palaeoenvironmental reconstruction and biogeographical implications, Quatern. Int., 302, 61–76, https://doi.org/10.1016/j.quaint.2012.11.036, 2013.

Lionello, P. (Ed.): The climate of the Mediterranean region: from the past to the future, 1st edn., Elsevier, London; Waltham, MA, 502 pp., ISBN: 978-0-12-416042-2, 2012.

Litt, T., Pickarski, N., Heumann, G., Stockhecke, M., and Tzedakis, P. C.: A 600,000 year long continental pollen record from Lake Van, eastern Anatolia (Turkey), Quaternary Sci. Rev., 104, 30–41, https://doi.org/10.1016/j.quascirev.2014.03.017, 2014.

Ludwig, K. R. and Paces, J. B.: Uranium-series dating of pedogenic silica and carbonate, Cratere Flat, Nevada, Geochim. Geochosmochim. Ac., 66, 487–506, 2002.

Margari, V., Skinner, L. C., Tzedakis, P. C., Ganopolski, A., Vautravers, M., and Shackleton, N. J.: The nature of millennial-scale climate variability during the past two glacial periods, Nat. Geosci., 3, 127–131, https://doi.org/10.1038/ngeo740, 2010.

Martìn-Algarra, A., Martìn-Martìn, M., Andreo, B., Julià, R., and González-Gómez, C.: Sedimentary patterns in perched spring travertines near Granada (Spain) as indicators of the paleohydrological and paleoclimatological evolution of a karst massif, Sediment. Geol., 161, 217–228, https://doi.org/10.1016/S0037-0738(03)00115-5, 2003.

Mercier, N., Hatté, C., Fontugne, M., Reyss, J.-L., Valladas, H., Wengler, L., Brugal, J.-P., Ouammou, A., and Weisrock, A.: Chronology of Upper Pleistocene sequences at Sidi Messaoud (wadi Noun, southwestern Morocco) based on ^{14}C, optical and U-series dating, Quat. Geochronol., 4, 326–334, https://doi.org/10.1016/j.quageo.2009.02.019, 2009.

New, M., Hulme, M., and Jones, P.: Representing Twentieth-Century Space–Time Climate Variability. Part II: Development of 1901–96 Monthly Grids of Terrestrial Surface Climate, J. Climate, 13, 2217–2238, https://doi.org/10.1175/1520-0442(2000)013<2217:RTCSTC>2.0.CO;2, 2000.

Nicod, J.: Sources et hydrosystèmes karstiques des régions arides et semi-arides. Essai géographique, Karstologia, 35, 47–58, https://doi.org/10.3406/karst.2000.2458, 2000 (in French).

North Greenland Ice Core Project members: High-resolution record of Northern Hemisphere climate extending into the last interglacial period, Nature, 431, 147–151, https://doi.org/10.1038/nature02805, 2004.

Ollivier, V., Guendon, J.-L., Ali, A., Roiron, P., and Ambert, P.: Evolution postglaciaire des environnements travertineux provençaus et alpins: nouveau cadre chronologique, faciès et dynamiques morphosédimentaires, Quaternaire, 17, 51–67, 2006 (in French).

Pedley, H. M.: Classification and environmental models of cool freshwater tufas, Sediment. Geol., 68, 143–154, https://doi.org/10.1016/0037-0738(90)90124-C, 1990.

Pedley, M., Martín, J. A. G., Delgado, S. O., and García Del Cura, M. Á.: Sedimentology of Quaternary perched springline and paludal tufas: criteria for recognition, with examples from Guadalajara Province, Spain, Sedimentology, 50, 23–44, https://doi.org/https://doi-org.inee.bib.cnrs.fr/10.1046/j.1365-3091.2003.00502.x, 2003.

Pentecost, A.: British travertines: a review, P. Geologist. Assoc., 104, 23–39, https://doi.org/10.1016/S0016-7878(08)80152-6, 1993.

Pentecost, A.: The quaternary travertine deposits of Europe and Asia Minor, Quaternary Sci. Rev., 14, 1005–1028, https://doi.org/10.1016/0277-3791(95)00101-8, 1995.

Pentecost, A.: Travertine, Springer-Verlag, Berlin Heidelberg, 445 pp., https://doi.org/10.1007/1-4020-3606-X, 2005.

Pigati, J. S., McGeehin, J. P., Muhs, D. R., and Bettis, E. A.: Radiocarbon dating late Quaternary loess deposits using small terrestrial gastropod shells, Quaternary Sci. Rev., 76, 114–128, https://doi.org/10.1016/j.quascirev.2013.05.013, 2013.

Pla-Pueyo, S., Viseras, C., Henares, S., Yeste, L. M., and Candy, I.: Facies architecture, geochemistry and palaeoenvironmental reconstruction of a barrage tufa reservoir analog (Betic Cordillera, S. Spain), Non-Mar. Carbonates Multidiscip. Approach, 437, 15–36, https://doi.org/10.1016/j.quaint.2016.05.022, 2017.

Prado-Pérez, A. J., Huertas, A. D., Crespo, M. T., Sánchez, A. M., and Pérez Del Villar, L.: Late Pleistocene and Holocene mid-latitude palaeoclimatic and palaeoenvironmental reconstruction: an approach based on the isotopic record from a travertine formation in the Guadix-Baza basin, Spain, Geol. Mag., 150, 602–625, https://doi.org/10.1017/S0016756812000726, 2013.

Rousseau, L., Beauchamp, J., Bahain, J.-J., Boudad, L., Deschamps, P., Falguères, C., Ghaleb, B., Lartigot, A.-S., and Pozzi, J.-P.: Premiers résultats d'une étude pluridisciplinaire sur des

travertins quaternaires du Maroc, Quaternaire, 17, 343–350, https://doi.org/10.4000/quaternaire.913, 2006 (in French).

Rousseau, L., Falguères, C., Pozzi, J.-P., Weisrock, A., Ghaleb, B., Mahieux, G., Beauchamp, J., Ouammou, A., Haddad, M., Bejjit, L., Charif, A., and Lauriol, B.: Chronologie et enregistrements climatiques dans les dépôts travertineux du Maroc, L'Anthropologie, 121, 82–89, https://doi.org/10.1016/j.anthro.2017.03.009, 2017 (in French).

Sánchez Goñi, M., Cacho, I., Turon, J., Guiot, J., Sierro, F., Peypouquet, J., Grimalt, J., and Shackleton, N.: Synchroneity between marine and terrestrial responses to millennial scale climatic variability during the last glacial period in the Mediterranean region, Clim. Dyamn., 19, 95–105, https://doi.org/10.1007/s00382-001-0212-x, 2002.

Sánchez Goñi, M. F., Turon, J.-L., Eynaud, F., and Gendreau, S.: European Climatic Response to Millennial-Scale Changes in the Atmosphere–Ocean System during the Last Glacial Period, Quaternary Res., 54, 394–403, https://doi.org/10.1006/qres.2000.2176, 2000.

Sánchez Goñi, M. F., Landais, A., Fletcher, W. J., Naughton, F., Desprat, S., and Duprat, J.: Contrasting impacts of Dansgaard–Oeschger events over a western European latitudinal transect modulated by orbital parameters, Quaternary Sci. Rev., 27, 1136–1151, https://doi.org/10.1016/j.quascirev.2008.03.003, 2008.

Shackleton, N. J., Fairbanks, R. G., Chiu, T., and Parrenin, F.: Absolute calibration of the Greenland time scale: implications for Antarctic time scales and for $\Delta^{14}C$, Quaternary Sci. Rev., 23, 1513–1522, https://doi.org/10.1016/j.quascirev.2004.03.006, 2004.

Tzedakis, P. C. and Bennett, K. D.: Interglacial vegetation succession: A view from southern Europe, Quaternary Sci. Rev., 14, 967–982, https://doi.org/10.1016/0277-3791(95)00042-9, 1995.

Vaudour, J.: Introduction à l'étude des édifices travertineux holocènes, Méditerranée, 57, 3–10, https://doi.org/10.3406/medit.1986.2356, 1986 (in French).

Vaudour, J.: Évolution holocène des travertins de vallée dans le Midi méditéranéen français, Geogr. Phys. Quatern., 48, 315–326, 1994 (in French).

Wackenheim, Q., Limondin-Lozouet, N., Dabkowski, J., Boudad, L., and Berger, J.-F.: Reconstructing mid-Holocene palaeoenvironmental dynamic in the Middle Atlas (Morocco) inferred from non-marine molluscs succession of the Aït said ou Idder tufa sequence, Quaternaire, 31, 145–164, https://doi.org/10.4000/quaternaire.13783, 2020.

Weisrock, A.: Variations climatiques et périodes de sédimentation carbonatée à l'holocène, L'âge des dépôts, Méditerranée, 57, 165–167, https://doi.org/10.3406/medit.1986.2388, 1986 (in French).

Weisrock, A., Rousseau, L., Reyss, J.-L., Falguères, C., Ghaleb, B., Bahain, J.-J., Beauchamp, J., Boudad, L., Mercier, N., Mahieux, G., Pozzi, J.-P., and Abderrahmane Ouammou, N. J.-I.: Travertins de la bordure nord du Sahara marocain: dispositifs morphologiques, datations U/Th et indications paléoclimatiques, Géomorphologie, 14, 153–167, https://doi.org/10.4000/geomorphologie.6793, 2008 (in French).

Wengler, L. and Vernet, J.-L.: Vegetation, sedimentary deposits and climates during the Late Pleistocene and Holocene in eastern Morocco, Palaeogeogr. Palaeocl., 94, 141–167, https://doi.org/10.1016/0031-0182(92)90117-N, 1992.

Wolf, D., García-Tortosa, F. J., Richter, C., Dabkowski, J., Roettig, C. B., and Faust, D.: Holocene landscape evolution in the Baza Basin (SE-Spain) as indicated by fluvial dynamics of the Galera River, Quaternary Science Advances, 4, 100030, https://doi.org/10.1016/j.qsa.2021.100030, 2021.

Zielhofer, C., Fletcher, W. J., Mischke, S., De Batist, M., Campbell, J. F. E., Joannin, S., Tjallingii, R., El Hamouti, N., Junginger, A., Stele, A., Bussmann, J., Schneider, B., Lauer, T., Spitzer, K., Strupler, M., Brachert, T., and Mikdad, A.: Atlantic forcing of Western Mediterranean winter rain minima during the last 12,000 years, Quaternary Sci. Rev., 157, 29–51, https://doi.org/10.1016/j.quascirev.2016.11.037, 2017.